ELSEVIER

Journal of Organometallic Chemistry 577 (1999) 126–133

Journal of Organometallic Chemistry

Oxide bridged mixed metal organometallics: the reaction of $Ru_4(CO)_{13}[\mu_3\text{-}PN(R)_2]$ R = ^{i}Pr, Cy with $Cp^*W(O)_2CCPh$

John H. Yamamoto [a], Gary D. Enright [b], Arthur J. Carty [a,b,*]

[a] *Steacie Institute for Molecular Sciences, National Research Council of Canada, 100 Sussex Drive, Ottawa, Ontario K1A OR6, Canada*
[b] *Department of Chemistry, Ottawa–Carleton Chemistry Institute, University of Ottawa, Ottawa, Ontario K1N 6N5, Canada*

Received 16 October 1998

Abstract

The reaction of the tungsten oxo acetylide complex $Cp^*W(O)_2CCPh$ with $Ru_4(CO)_{12-13}[\mu_3\text{-}PN(R)_2]$ where R = ^{i}Pr or Cy affords two oxo bridged metal clusters η^5-$Cp^*W(\mu\text{-}O)Ru_4(CO)_9(\mu\text{-}CO)[\mu_3\text{-}\eta^2\text{-}P(O)N(R)_2](\mu_4\text{-}\eta^2\text{-}CCPh)$ (**2**) and η^5-$Cp^*W(\mu\text{-}O)_2Ru_4(CO)_{10}[\mu_3\text{-}PN(R)_2](\mu_4\text{-}\eta^2\text{-}CCPh)$ (**3**). X-ray analysis shows that **2** has a single W–O–Ru oxide bridge and contains the first example of a diisopropylaminophosphinidoxo ligand while in **3** both oxide ligands bridge W–Ru bonds. The reaction of **3** with $HBF_4 \cdot Et_2O$ forms the new W–F complex η^5-$Cp^*WF(\mu_3\text{-}O)HRu_4(CO)_9[\mu_3\text{-}\eta^2\text{-}P(O)N(R)_2](\mu_4\text{-}\eta^2\text{-}CCPh)$ (**4**).

Keywords: Phosphinidene; Phosphinidoxo; Tungsten; Ruthenium; Fluoride

1. Introduction

The oxide (=O) group is normally considered to be a hard ligand in organometallic chemistry, principally associated with early, high oxidation state metal fragments [1]. However, recent developments suggest that oxides can play an important role as interfacial ligands, bridging early-high and late-low oxidation state metals [2] to form mixed metal oxo clusters which may serve as models for oxide supported platinum metal catalysts [3]. In this paper we report the synthesis of several new oxide bridged early-late organometallic clusters. The strategy we have employed is to deliver an early metal oxo organometallic fragment to a late metal by using the well known affinity of late metals for unsaturated hydrocarbyls [4]. Although the number of early metal oxo compounds bearing unsaturated hydrocarbyl ligands is not very extensive, the molecule $Cp^*W(O)_2$-CCPh [5] has the appropriate functionality to coordinate to transition metal carbonyl complexes. On the other hand the *nido*-phosphinidene clusters $Ru_4(CO)_{13}(\mu_3\text{-}PR)$ are known to interact strongly with alkynes, forming a variety of stable complexes in which the acetylene coordinates on a square Ru_3P or Ru_4 face as a four-electron donor [6]. These two types of molecules thus appear ideal to test the synthetic strategy outlined above. The reaction of $Cp^*W(O)_2CCPh$ with $Ru_4(CO)_{13}[\mu_3\text{-}PN(R)_2]$ (**1**) in refluxing hexane produced two types of oxide containing organometallic clusters, one of which, η^5-$Cp^*W(\mu\text{-}O)Ru_4(CO)_9(\mu\text{-}CO)[\mu_3\text{-}\eta^2\text{-}P(O)N(R)_2](\mu_4\text{-}\eta^2\text{-}CCPh)$ (**2**) has W–O–Ru and W–O–P interactions and contains the rare phosphinidoxo ligand RPO [3]. The other η^5-$Cp^*W(\mu\text{-}O)_2Ru_4(CO)_{10}[\mu_3\text{-}PN(R)_2](\mu_4\text{-}\eta^2\text{-}CCPh)$ (**3**) possesses two oxide ligands bridging Ru–W bonds. Subsequent reaction of **2** with $HBF_4 \cdot Et_2O$ formed the new complex η^5-$Cp^*WF(\mu_3\text{-}O)HRu_4(CO)_9[\mu_3\text{-}\eta^2\text{-}P(O)N(R)_2](\mu_4\text{-}\eta^2\text{-}CCPh)$ (**4**) with a W–F bond.

* Corresponding author.

0022-328X/99/$ - see front matter
PII: S0022-328X(98)01037-7

2. Results and discussion

A potentially powerful methodology for constructing oxide bridged mixed metal clusters consists of delivering an early metal oxo compound bearing an unsaturated hydrocarbyl group to a late metal with an affinity for hydrocarbyl π-electrons [4]. Using this strategy, reaction of η^5-Cp*W(O)$_2$CCPh (Cp* = C_5Me_5) [4] in refluxing hexane for 3 h with the *nido* 62e- phosphinidene cluster $Ru_4(CO)_{13}[\mu_3\text{-}PN(^iPr)_2]$ known to strongly coordinate acetylenes, afforded two new complexes η^5-Cp*W(μ-O)Ru$_4$(CO)$_9$(μ-CO)[μ_3-η^2-P(O)N-(^{i}Pr)$_2$](μ_4-η^2-CCPh) (**2a**) and η^5-Cp*W(μ-O)$_2$Ru$_4$-(CO)$_{10}$[μ_3-PN(^{i}Pr)$_2$](μ_4-η^2-CCPh) (**3**) in 57 and 32% yield, respectively. Similar compounds were formed but in quite different proportions when $Ru_4(CO)_{13}[\mu_3$-PN(Cy)$_2$] was used, with yields of 18.8 and 51.3% for compounds **2b** and **3b**, respectively.

In refluxing heptane (30 min), **3a**,**b** are converted solely to **2a**,**b** whereas **2** remains unchanged (Scheme 1). Thus, **3** with two W–O–Ru bridges (vide infra) appears to be an intermediate in the reaction of Cp*W(O)$_2$C$_2$Ph with **1**. Cluster **2** on the other hand, in which oxidation of a phosphinidene ligand by a tungsten oxo functionality has occurred, is the thermodynamic product of this reaction. The rearrangement of **2** to **3** can be described in terms of the cleavage of two P–Ru bonds, the formation of bonds between P and Ru1 the formation of a hinge of the butterfly cluster between Ru2 and Ru4 and the oxidative addition of O1 to P to form the PO bond. The above rearrangement is accomplished by a rotation of the acetylide ligand on the WRu$_4$ framework of **3** such that the tungsten atom which is bonded to the tail [C(2)Ph] of the acetylide in **3** is attached in a η^1-fashion to the head [C(1)] in **2**. It is perhaps surprising, that in intermediate **3**, the head of the acetylide is not attached to tungsten, as in the precursor molecule Cp*W(O)$_2$CCPh. However, acetylide bond isomerisation and structural rearrangements have been observed previously in mixed metal systems [7] and such transformations are more likely than the alternative of phenyl group transfer between acetylide carbon atoms.

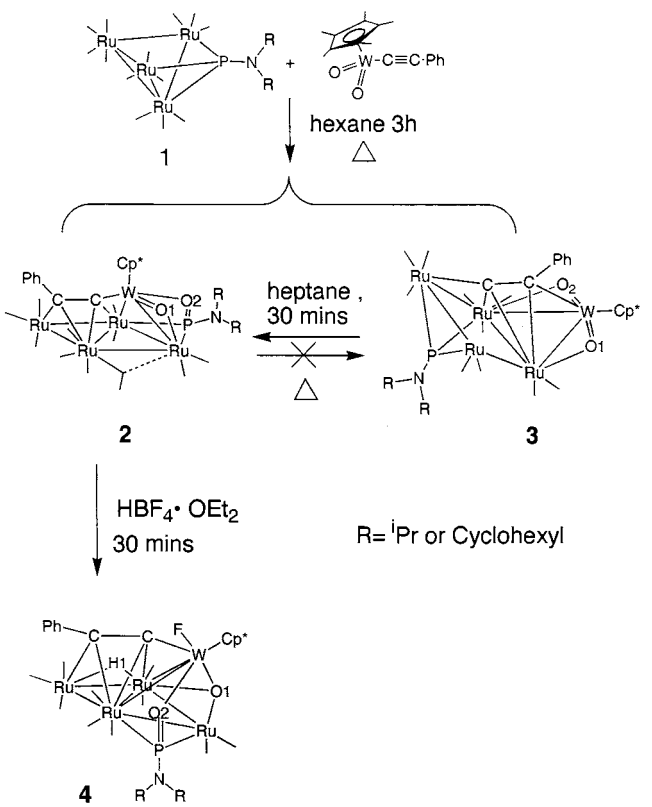

Scheme 1.

As we have demonstrated elsewhere, the treatment of transition metal clusters containing the diisopropylaminophosphinidene group with HBF$_4$ · OEt$_2$ followed by hydrolysis causes oxidation of the phosphorus atom to a PO ligand [8,9]. With this in mind compound **2** was treated with an excess of HBF$_4$ · OEt$_2$. However, the anticipated reaction did not occur and a new compound **4,** η^5-Cp*WF(μ_3-O)HRu$_4$(CO)$_9$[μ_3-η^2-P(O)N-(^{i}Pr)$_2$](μ_4-η^2-CCPh) with a W–F bond was isolated in 38% yield. The presence of tungsten fluorine bonds in **4** was verified via ^{19}F-NMR spectroscopy. The ^{19}F spectrum of **4a** contained a doublet at −59.44 ppm with $^3J_{P-F}$ of 15.26 Hz for **4a** and for **4b** a doublet at −59.23 ppm with $^3J_{P-F}$ of 13.73 Hz. Though it is not unusual for an organometallic tungsten center in a high oxidation state to react with a fluorinating reagent [10], complex **4a** is the first organometallic mixed metal cluster to contain a fluoride ligand [10].

HBF$_4$ · Et$_2$O has been previously used as a fluorinating agent for tungsten metal centers. For example the treatment of WH$_6$(PPhMe$_2$)$_2$ with HBF$_4$ · Et$_2$O in the presence of CO leads to the cationic cluster [W$_2$(μ-F)$_3$(CO)$_4$(PPhMe$_2$)$_4$][BF$_4$] [11]. The formation of a metal–fluoride bond via reaction between a metal carbonyl and a fluorinating agent has been the subject of two recent review articles [10].

The molecular structure of **2a** (Fig. 1) consists of an almost planar Ru$_4$ butterfly (dihedral angle of 177.43°) with the Cp*WC$_2$Ph fragment coordinated as a 4e-donor on the Ru(2)Ru(3)Ru(4) triangle as a μ3-η2-||-acetylene and with the tungsten atom asymmetrically bridging the Ru(1)–Ru(2) bond (Ru(1)–W = 2.9248(3); Ru(2)–W = 2.7823(3) Å). The most interesting features of the cluster are associated with the oxide ligands derived from the Cp*W(O)$_2$ moiety. One oxygen atom, O(2) acts as a bridge between tungsten and the phosphorus atom of the phosphinidene of **1a** forming a μ_3-η^2 diisopropylaminophosphinidoxo[O=PN(^{i}Pr)$_2$] ligand on the Ru(1)–Ru(2)–W face. The P–O(2) bond length (1.570(1) Å) is comparable to that (P–O = 1.53(1)) in Fe$_3$(CO)$_{10}$(μ_3-RPO) (R = ^{i}Pr or ^{t}Bu) the only

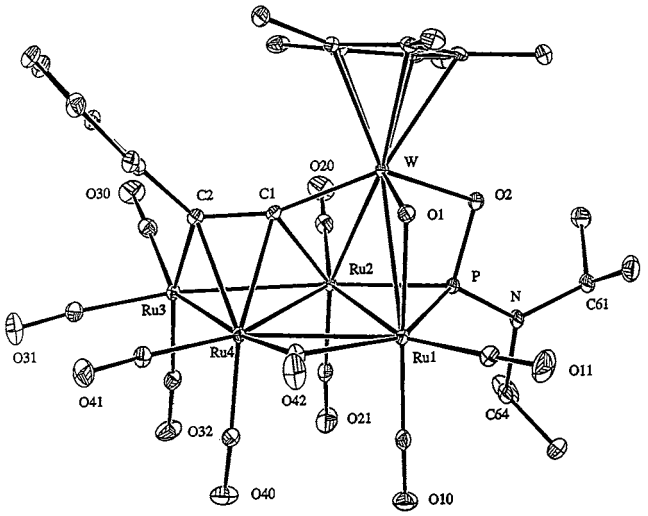

Fig. 1. An ORTEP diagram of η^5-Cp*W(μ-O)$Ru_4(CO)_9$(μ-CO)[μ_3-η^2-OPN(^{i}Pr)$_2$](μ_4-η^2-CCPh) **2a** showing 30% probability thermal ellipsoids. Hydrogen atoms are omitted for clarity. Selected bond lengths not mentioned in the text (Å): W–Ru(1) = 2.9248(3), W–Ru(2) = 2.7823(1), Ru(1)–Ru(2) = 2.8428(4), Ru(1)–Ru(4) = 2.8306(4), Ru(2)–Ru(3) = 2.8802(4), Ru(2)–Ru(4) = 2.7587(4), Ru(3)–Ru(4) = 2.6882(4) and angles (°) O(1)–W–O(2) = 96.5(1), N–P–O(2) = 106.1(1).

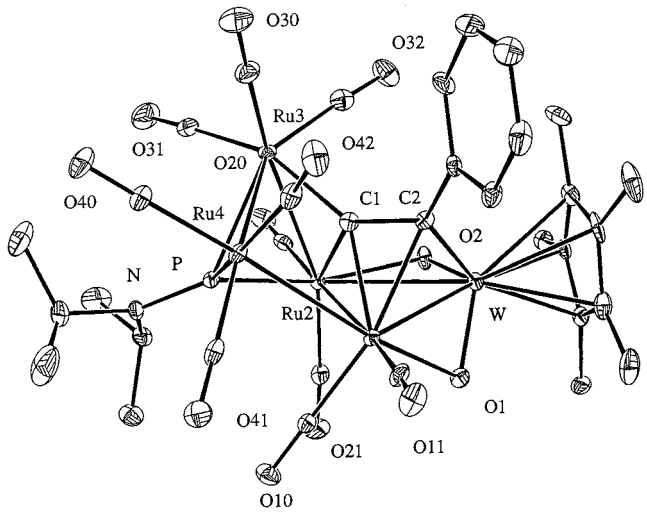

Fig. 2. An ORTEP diagram of η^5-Cp*W(μ-O)$_2Ru_4(CO)_{10}$(μ_3-PN(^{i}Pr)$_2$)(μ_4-η^2-CCPh) **3a** showing 30% probability thermal ellipsoids. Hydrogen atoms are omitted for clarity. Selected bond lengths not mentioned in the text (Å): W–Ru(1) = 2.6910(5), W–Ru(2) = 3.0467(5), Ru(1)–Ru(2) = 2.8154(7), Ru(1)–Ru(4) = 2.8661(6), Ru(2)–Ru(3) = 2.7786(6), Ru(3)–Ru(4) = 2.8393(7) and angles (°) O(1)–W–O(2) = 111.0(2).

other known μ-RPO complexes [12] and is only slightly longer than the PO distances in typical phosphine oxide complexes (e.g. P=O = 1.4382(2) Å in Ph_3PO) [13]. Together with the long W–O(2) distance (2.07(2) Å) indicative of a W–O single bond this suggests a P=O→W interaction. Cluster **2a** also has a W–O(1)–Ru(1) bridge (W–O(1) = 1.759(2); Ru(1)–O(1) = 2.227(2) Å) but in this case the oxide is double bonded to the tungsten and the bonding is best described as W=O→Ru. In this model W is in a +4 oxidation state and one of the original oxo ligands has transferred to and oxidized the phosphinidene ligand. Overall **2** is electron precise (76 e-, 7 M–M) (Table 2).

In the second cluster **3a** (Fig. 2) the Cp*W$(O)_2C_2$Ph fragment is attached to a non-planar arrangement of four ruthenium atoms (4Ru–Ru) via a μ_4-acetylene, two W–Ru bonds and two W–O–Ru oxide bridges. From the W–O and Ru–O bond lengths (W–O(1) = 1.815(4); W–O(2) = 1.783(4); Ru(1)–O(1) = 2.147(4); Ru(2)–O(2) = 2.191(4) Å), the metal-oxide interaction is best represented as W=O→Ru for both bridging oxides. In this case the tungsten atom is formally in a +6 oxidation state. Complex **3** is the first example of an early-late metal organometallic cluster with two oxide bridges to ruthenium. Overall **3** is electron rich (80 e-, 6 M–M). The tetrahedral organometallic cluster $CpWOs_3(CO)_9(\mu\text{-}O)_2(\mu\text{-}H)$ with two bridging oxides would be counted as a 62 electron system and therefore also electron rich if both oxides donated four-electrons. However, the authors have counted each of the bridging oxide ligands as three-electron donors to account for the 60 electrons predicted by the effective atomic number rule [2e]. To accommodate this, the bonding is thought to be best described as intermediate between the forms W=O→Os and W–O–Os where the latter represents an ether-like link between the two metals (Table 3).

The structure of **4a** (Fig. 3) consists of four ruthenium atoms arranged in a butterfly configuration (dihe-

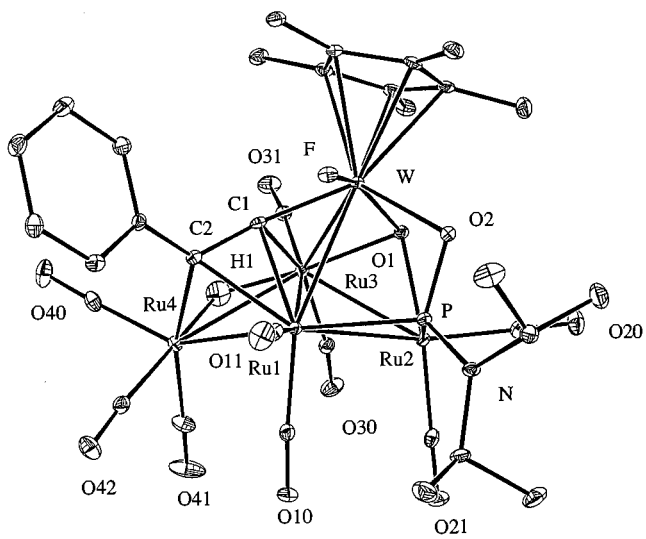

Fig. 3. An ORTEP diagram of η^5-Cp*WF(μ-O)$HRu_4(CO)_9$(μ-CO)(μ_3-η^2-OPN(^{i}Pr)$_2$)(μ_4-η^2-CCPh) **4a** showing 30% probability thermal ellipsoids. Hydrogen atoms are omitted for clarity. Selected bond lengths not mentioned in the text (Å): W–Ru(1) = 2.8740(4), W–Ru(3) = 2.8895(4), Ru(1)–Ru(3) = 2.7857(5), Ru(1)–Ru(4) = 2.7685(4), Ru(2)–Ru(3) = 2.7686(4), Ru(3)–Ru(4) = 2.2.9271(4), W–F 1.973(2).

dral angle for Ru(2)–Ru(3)–Ru(1)–Ru(4) = −138.58°) with the tungsten atom of the Cp*W(O)$_2$-CCPh ligand bridging a hinge of the butterfly. The distance between W and Ru(2) is 3.4269(5) Å which is much longer than the sum of the covalent radii of W (1.3) and Ru (1.33) [14]. This indicates that the tungsten atom and Ru(2) are not within bonding distance. The acetylide ligand caps a triangular face of the butterfly. The atom O(1) triply bridges W, Ru(3) and Ru(2)[W–O(1) = 1.955(2), Ru(3)–O(1) = 2.116(2), Ru(2)–O(1) = 2.061 (2) Å]. This type of μ_3-oxide ligand bridging mixed metals is not uncommon and has been observed before in related systems [15]. In this environment the W atom is best described as being in a formal oxidation state of +4. The aminophosphinidoxo ligand triply bridges Ru(1), Ru(2) and W. The phosphorus atom lies across the edge formed by Ru(1) and Ru(2) and O(2) is η^1 bound to the tungsten atom. The P–O(2) bond distance is 1.559 (2) Å which is indicative of a phosphorus oxygen double bond. For comparison the P=O bond distance of Ph_3PO is 1.4383(2) Å [13]. Together with the long W–O(2) distance (2.116(2) Å) which is indicative of a W–O single bond, this suggests a P=O→W interaction. With this coordination mode the phosphinidoxo ligand is formally donating 4e-. The phosphinidoxo ligand observed in **4a** is very similar to the phosphinidoxo ligand in **3a** (vide-infra). An η^1-fluoride ligand is attached to the tungsten atom adjacent to both O(2) and C(1). The hydride ligand bridging Ru3 and Ru4 was located in an electron density map and its position was refined isotropically. The existence of a hydride ligand was also confirmed by the observation of a singlet resonance in the proton NMR spectrum at −20.54 ppm which is a typical chemical shift for a bridging hydride. Overall **4** is electron precise (76 e-, 7 M–M) (Table 4).

Addition of fluoride ion to the tungsten center initiates a rearrangement of the metal framework. This rearrangement can be accounted for by the cleavage of the butterfly hinge bond (Ru4–Ru2), and the W–Ru1 bond, as well as the transformation of the bridging carbonyl to a terminal one. Concurrently, a new hinge bond is formed between Ru1–Ru3 and bonds are generated between W–Ru4 and O1–Ru4. A bridging hydride is also incorporated between Ru3 and Ru4.

In summary, new types of stable oxide bridged mixed metal organometallic clusters can be accessed via reaction of high oxidation state oxo acetylides with late metal carbonyl complexes. We are currently examining the potential of this methodology for the introduction of oxide ligands into other mixed oxidation state organometallic clusters and for the generation of new oxidized phosphide supporting ligands.

3. Experimental

3.1. General data

Unless specified otherwise, all reactions were carried out under an atmosphere of nitrogen. All solvents were appropriately dried prior to use. $HBF_4 \cdot Et_2O$ was purchased from Aldrich and used without further purification. $Ru_4(CO)_{13}[\mu_3\text{-}PN(^iPr)_2]$ [3], $Ru_4(CO)_{12}[\mu_3\text{-}PN(^iPr)_2]$ [8], $Ru_4(CO)_{13}[\mu_3\text{-}PN(Cy)_2]$ [16] and Cp*W(O)$_2$CCPh [5] were synthesized by known procedures. TLC separations were performed in air using silica gel plates (60 A F254) (Merck, 0.25 nm). Elemental analysis was carried out by Ann Webb of the Institute of Biological Sciences of the National Research Council of Canada ^{19}F- and ^{31}P-NMR spectra were obtained with a Bruker DBX-500 at 474.50 or 202.54 MHz, respectfully. IR spectra were recorded on a Bio-Rad FTS-40A FTIR spectrometer.

3.2. Reaction of $Ru_4(CO)_{13}[\mu_3\text{-}PN(^iPr)_2]$ with Cp*W(O)$_2$CCPh

To 25 mg of $Ru_4(CO)_{13}[\mu_3\text{-}PN(^iPr)_2]$ (**1a**) (0.028 mmol) in a Schlenk tube was placed 13 mg of Cp*W(O)$_2$CCPh (0.029 mmol) and 25 ml of dry hexane. The mixture was refluxed for 3 h by which time the solution had turned to a dark red–brown color. The solution was dried in vacuo, and three compounds were separated by TLC in air with a 1:2 CH_2Cl_2 + hexane mixture. The compounds were in order of elution: $Ru_3(CO)_{12}$ (1 mg, 5.7%), $Ru_5(CO)_{13}[\mu_4\text{-}PN(^iPr)_2]$ (1 mg, 5.6%) and Cp*W(μ-O)$Ru_4(CO)_9$(μ-CO)[μ_3-η^2-OPN(^{i}Pr)$_2$](μ_4-η^2-CCPh) (18 mg, 57%); **2a**. The base line was then eluted with pure CH_2Cl_2 and an orange band was isolated. This band contained Cp*W(μ-O)$_2Ru_4(CO)_9[\mu_3\text{-}PN(^iPr)_2](\mu_4\text{-}\eta^2\text{-}CCPh)$ (10 mg, 0.0089 mmol, 32%); **3a**. Spectral data for Cp*W(μ-O)$Ru_4(CO)_9$(μ-CO)[μ_3-η^2-OPN(^{i}Pr)$_2$](μ_4-η^2-CCPh) **2a**: IR, (ν (CO) in hexane), 2065(s), 2027(s), 2015(vs), 2001(m), 1981(m), 1965(w), 1960(vw) cm^{-1}. IR, (ν (CO) in CH_2Cl_2), 2060(s), 2022(vs), 2009(s), 1994(m), 1976(m), 1957(w), 1985(w) cm^{-1}. ^{1}H-NMR, (δ in $CDCl_3$), 7.80 (1H, d, J_{H-H} = 7.9), 7.49 (1H, dd, J_{H-H} = 6.7, J_{H-H} = 7.9), 7.20 (2H, dd, J_{H-H} = 7.9, J_{H-H} = 7.4), 7.20 (1H, dd, J_{H-H} = 6.7, J_{H-H} = 7.9), 6.78 (1H, d, J_{H-H} = 7.4), 3.88 (1H, q, J_{H-H} = 6.8), 3.75 (2H, q, J_{H-H} = 6.8), 2.00 (s, 15H), 1.43 (6H, d, J_{H-H} = 6.8), 1.37 (6H, d, J_{H-H} = 6.8). ^{31}P-NMR, (δ in $CDCl_3$), 248(s). Anal. Calc. for **2a**: C, 32.11, H, 2.70, N, 1.10. Found: C, 31.40, H, 2.61, N, 1.36%. Spectral data for Cp*W(μ-O)$_2Ru_4(CO)_9[\mu_3\text{-}PN(^iPr)_2](\mu_4\text{-}\eta^2\text{-}CCPh)$ **3a**: IR, (ν (CO) in hexane), 2071(s), 2036(s), 2021(vs), 2006(s), 1986(m), 1966(w), 1949(m) cm^{-1}. IR, (ν (CO) in CH_2Cl_2), 2070(m), 2036(s), 2016(vs), 2002(m), 1994(m), 1958(w), 1939(w) cm^{-1}. ^{1}H-NMR, (δ in

$CDCl_3$), 8.55 (1H, d, $J_{H-H} = 7.6$), 7.59 (1H, dd, $J_{H-H} = 6.9$, $J_{H-H} = 7.4$), 7.19 (2H, m), 6.19 (1H, d, $J_{H-H} = 7.4$), 3.92 (2H, m), 1.83 (s, 15H), 1.30(d, 15H, $J_{H-H} = 6.83$). ^{31}P-NMR, (δ in $CDCl_3$), 356 (bs). Anal. Calc. for **3a**: C, 31.92, H, 2.60, N, 1.13. Found: C, 31.81, H, 2.35, N, 1.21%.

3.3. Reaction of $Ru_4(CO)_{12}[\mu_3\text{-}PN(^iPr)_2]$ with $Cp^*W(O)_2CCPh$

To 18 mg of $Ru_4(CO)_{12}[\mu_3\text{-}PN(^iPr)_2]$ (0.021 mmol) in a Schlenk tube was placed 9 mg of $Cp^*W(O)_2CCPh$ (0.020 mmol) and 25 ml of dry hexane. The solution was refluxed for 3 h by which time the solution had turned to a dark red–brown color. The solution was dried in vacuo, and three compounds were separated by TLC in air with a 1:2 CH_2Cl_2 + hexane mixture as an eluting solvent system. The compounds were in order of elution: $Ru_3(CO)_{12}$ (1 mg, 7.6%), $Ru_5(CO)_{13}[\mu_4\text{-}PN(^iPr)_2]$ (2 mg, 8.6%) and **2a** (10 mg, 0.0089 mmol, 42%). The base line was then eluted with pure CH_2Cl_2 an a orange band was isolated. This band was determined to be **3a** (8 mg, 0.0071 mmol, 34%).

3.4. Reaction of $Ru_4(CO)_{13}[\mu_3\text{-}PN(Cy)_2]$ with $Cp^*W(O)_2CCPh$

To 400 mg of $Ru_4(CO)_{13}[\mu_3\text{-}PN(Cy)_2]$ **1b** (0.40 mmol) in a Schlenk tube was placed 184 mg of $Cp^*W(O)_2CCPh$ (0.40 mmol) and 25 ml of dry hexane. The solution was refluxed for 3 h by which time the solution was a dark red–brown color. The solution was dried in vacuo. Three compounds were separated by TLC in air with a 1:2 CH_2Cl_2 + hexane mixture. The compounds were in order of elution: $Ru_3(CO)_{12}$ (23 mg, 9.0%), $Ru_5(CO)_{15}[\mu_4\text{-}PN(Cy)_2]$ (35 mg, 7.7%), and $Cp^*W(\mu\text{-}O)Ru_4(CO)_9(\mu\text{-}CO)[\mu_3\text{-}\eta^2\text{-}P(O)N(Cy)_2](\mu_4\text{-}\eta^2\text{-}CCPh)$ (89 mg, 0.07 mmol, 18.8%) **2b**. The base line was then eluted with pure CH_2Cl_2 and an orange band was isolated. This band was determined to be $Cp^*W(\mu\text{-}O)_2Ru_4(CO)_9[\mu_3\text{-}PN(Cy)_2](\mu_4\text{-}\eta^2\text{-}CCPh)$ **3b** (243 mg, 0.20 mmol, 51.3%). Spectral data for $Cp^*W(\mu\text{-}O)Ru_4(CO)_9(\mu\text{-}CO)[\mu_3\text{-}\eta^2\text{-}P(O)N(Cy)_2](\mu_4\text{-}\eta^2\text{-}CCPh)$ **2b**: IR, (ν (CO) in hexane), 2064(s), 2027(s), 2014(vs), 2000(m), 1980(m), 1965(w), 1959(w), 1937(vw), 1890(w) cm^{-1}. ^{1}H-NMR, (δ in $CDCl_3$), 7.81(d, 1H, $J_{H-H} = 8.5$), 7.49(t, 1H, $J_{H-H} = 8.2$, $J_{H-H} = 8.5$), 7.22 (t, 1H, $J_{H-H} = 8.2$, $J_{H-H} = 7.4$), 7.14 (t, 1H, $J_{H-H} = 7.8$, $J_{H-H} = 7.4$), 6.78 (d, 1H, $J_{H-H} = 7.8$), 3.45 (m, 2H), 2.01 (s, 15H), 1.85–1.09 (m, 20H). ^{31}P-NMR, (δ in $CDCl_3$), 247(s). Anal. Calc. for **2b**: C, 34.48, H, 3.20, N, 1.06. Found: C, 34.01, H, 2.85, N, 1.15%. Spectral data for $Cp^*W(\mu\text{-}O)_2Ru_4(CO)_9[\mu_3\text{-}PN(Cy)_2](\mu_4\text{-}\eta^2\text{-}CCPh)$ **3b**: IR, (*v* (CO) in hexane), 2070(w), 2036(s), 2020(vs), 2004(m), 1995(m), 1985(w), 1965(vw), 1948(m) cm^{-1}. ^{1}H-NMR, (δ in $CDCl_3$), 8.60 (d, 1H, $J_{H-H} = 7.85$), 7.24 (dd, 2H, $J_{H-H} = 7.32$, $J_{H-H} = 7.38$), 7.15 (dd, 1H, $J_{H-H} = 7.34$, $J_{H-H} = 6.90$), 6.23 (d, 1H, $J_{H-H} = 7.79$) 3.56 (m, 2H), 1.85 (s, 15H), 1.82–1.32 (m, 20H). ^{31}P-NMR, (δ in $CDCl_3$), 364 (bs). Anal. Calc. for **3b**: C, 34.30, H, 3.27, N, 1.08. Found: C, 34.45, H, 3.54, N, 1.34%.

3.5. Thermolysis of *2a*

To 25 mg of **2a** (0.019 mmol) in a Schlenk tube was placed 20 ml of dry heptane and the red–brown solution was refluxed for 3 h. The reaction was then dried in vacuo and the crude solid was separated on a silica TLC plate with a 1:2 CH_2Cl_2 + hexane solvent system. Two compounds were isolated: $Ru_3(CO)_{12}$ (1 mg, 7.9%) and compound **2a** (8 mg, 0.063 mmol, 32%).

3.6. Thermolysis of *3a*

In a Schlenk tube 23 mg of **3a** (0.0186 mmol) was mixed with 20 ml of dry heptane and the orange solution was then refluxed for 30 min. The red–brown reaction mixture was then dried in vacuo and the crude material was then separated on a silica TLC plate with a 1:2 CH_2Cl_2 + hexane solvent system. Two compounds were separated: $Ru_3(CO)_{12}$ (1 mg, 8.4%) and compound **2a** (17 mg, 0.0139 mmol, 72%).

3.7. Thermolysis of *2b*

As described above for **2a**, 182 mg of **2b** (0.1375 mmol) and 20 ml of dry heptane were refluxed for 3 h. The red–brown reaction mixture was then dried in vacuo and the crude products were separated on a silica TLC plate with a 1:2 CH_2Cl_2 + hexane solvent system. Two compounds were isolated: $Ru_3(CO)_{12}$ (5 mg, 5.6%) and compound **2b** (130 mg, 0.0982 mmol, 71%).

3.8. Thermolysis of *3b*

Refluxing an orange solution of 140 mg of **3b** (0.1080 mmol) and 10 ml of dry heptane for 30 min gave a red–brown solution. The reaction mixture was then dried in vacuo and separation of the compounds on a silica TLC plate with a 1:2 CH_2Cl_2 + hexane solvent system afforded two compounds: $Ru_3(CO)_{12}$ (1 mg, 1.4%) and compound **2b** (97 mg, 0.0733 mmol, 68%).

3.9. Reaction of *2a* with $HBF_4 \cdot Et_2O$

A CH_2Cl_2 solution of **2a** (80 mg, 0.063 mmol) was stirred under an atmosphere of nitrogen gas at 25°C for 24 h with 100 μl of $HBF_4 \cdot Et_2O$. The solution was then dried in-vacuo and the dark red residue was placed on to a silica gel plate. A 50:50 CH_2Cl_2 + hexane solution was used as the eluting solvent and a single compound

Table 1
Crystallographic data for compounds **2a**, **3a** and **4a**

Formula	$WRu_4PO_{12}NC_{34}H_{34}$	$WRu_4PO_{12}NC_{34}H_{34} \cdot CH_2Cl_2$	$WRu_4PFO_{11}NC_{33}H_{35}$
Formula weight	1267.73	1352.69	1258.72
Crystal system	Monoclinic	Triclinic	Triclinic
a (Å)	13.0014(2)	11.2133(1)	11.5202(1)
b (Å)	21.4552(3)	12.0983(1)	11.4924(1)
c (Å)	14.7878(3)	16.9326(1)	16.3814(2)
α (°)	90	73.04(1)	91.91(1)
β (°)	107.96(1)	87.20(1)	108.58(1)
γ (°)	90	74.75(1)	108.35(1)
V (Å^3)	3924.1(1)	2118.87(3)	1926.52(6)
Crystal dimensions(mm)	$0.20 \times 0.20 \times 0.20$	$0.03 \times 0.15 \times 0.20$	$0.150 \times 0.150 \times 0.045$
Space group	$P2_1/n$ (no. 14)	$P\bar{1}$ (no. 2)	$P\bar{1}$ (no. 2)
Z value	4	2	2
$\rho_{calc.}$ (Mg m^{-3})	2.14	2.12	2.17
μ (Mo–K_α) (mm^{-1})	4.53	4.35	4.61
T (°C)	−150	−150	−150
$2\Theta_{max}$ (°)	57.3	57.5	57.5
No. of reflections measured	27168	17866	22519
No. of unique reflections	10104	10556	9835
No. of reflections observed [$I > 2.5\sigma(I)$]	8270	8203	8400
No. of variables	615	506	469
Goodness-of-fit	0.92	1.26	1.43
Max shift in final cycle	0.00	0.163	0.00
Residuals: R; R_w	0.025; 0.028	0.038; 0.043	0.025;0.026
Abs. Cor.	Empirical	Empirical	Empirical
Largest peak in final difference map (e Å^{-2})	1.59	2.08	1.20

was isolated η^5-Cp*WF(μ_3-O)HRu$_4$(CO)$_9$[μ_3-η^2-P(O)N(^{i}Pr)$_2$](μ_4-η^2-CCPh) **4** (23 mg, 0.018 mmol, 28%). Spectral data for **4a**: IR, (ν (CO) in CH_2Cl_2), 2080(s), 2038 (vs), 1999(s), 1982 (sh), 1953(m), 1929(w) cm^{-1}. ^{1}H-NMR, (δ in $CDCl_3$), 7.83 (d, 2H, $J_{H-H} = 7.38$), 7.61 (dd, 1H, $J_{H-H} = 7.50$, $J_{H-H} = 7.38$), 7.51 (dd, 2H, $J_{H-H} = 7.50$, $J_{H-H} = 7.38$) 3.51 (m, 2H), 2.32 (s, 15H), 1.28 (m, 6H) -20.4 (1H, s). ^{31}P-NMR, (δ in $CDCl_3$), 315 (s). ^{19}F-NMR, (δ in $CDCl_3$ vs. CF_3COOH), −59.44 (d, $^3J_{P-F} = 15.26$). Anal. Calc. for **4a**: C, 31.71, H, 2.74, N, 1.09. Found: C, 31.43, H, 2.85, N, 1.23%.

3.10. Reaction of *2b* with $HBF_4 \cdot Et_2O$

A CH_2Cl_2 solution of **2b** (56 mg, 0.042 mmol) was stirred under an atmosphere of nitrogen gas at RT for 30 min with 100 μl of $HBF_4 \cdot Et_2O$. The solution was then dried in vacuo and the dark red residue was placed on to a silica gel plate. A 50:50 CH_2Cl_2 + hexane solution was used as the eluting solvent affording a single product. η^5-Cp*WF(μ_3-O)HRu$_4$(CO)$_9$[μ_3-η^2-P(O)N(^{i}Pr)$_2$](μ_4-η^2-CCPh) **4b**. (22 mg, 0.0164 mmol 39%). Spectral data for **4b**: IR, (ν (CO) in hexane), 2080(s), 2018(vs), 2000(s), 1983(sh), 1953(m), 1929(w) cm^{-1}. ^{1}H-NMR, (δ in $CDCl_3$), 7.77 (d, 2H, $J_{H-H} =$ 7.7), 7.33 (t, 2H, $J_{H-H} = 7.3$, $J_{H-H} = 7.7$), 7.25 (t, 2H, $J_{H-H} = 7.3$, $J_{H-H} = 7.9$), 3.21 (m, 2H), 2.19 (s, 15H), 1.72-1.26 (m, 20H) −21.4 (1H, s). ^{31}P-NMR, (δ in $CDCl_3$), 188(s). ^{19}F-NMR, (δ in $CDCl_3$ versus CF_3COOH), −59.23 (d, $^3J_{P-F} = 13.73$). Anal. Calc. for **4b**: C, 33.96, H, 3.23, N, 1.04. Found: C, 33.63, H, 3.58, N, 0.96%.

3.11. Crystallographic analyses

Orange crystals of **3a** suitable of X-ray diffraction analysis were grown by slow evaporation of a 1:2 CH_2Cl_2 + hexane solution at −20°C. Red crystals of **2a** and **4a** suitable for X-ray diffraction analysis were grown from benzene and hexane solutions, respectively, at 20°C. The crystals used in the diffraction measurements were mounted on a glass fiber with 5 min epoxy. Diffraction measurements were made on a Siemens SMART CCD automatic diffractometer by using graphite-monochromated Mo–K_α radiation. The unit cells were determined from randomly selected reflections obtained by using the SMART CCD automatic search, center, index and least-square routines. Crystal data, data collection parameters, and results of the analyses are listed in Table 1. All data processing was performed on a silicon graphics INDY computer by using the NRCVAX [17] structure solving library obtained from the National Research Council of Canada, Ottawa, Ontario. Neutral atom scattering factors were calculated by the standard procedures [18]. Anomalous dispersion corrections were applied to all non-hydrogen atoms [19]. Lorentz/polarization (Lp) and absorption corrections were applied to the data for the structure

Table 2
Selective intramolecular bond lengths (Å) and angles (°) for η^5-Cp*W(μ-O)$Ru_4(CO)_9$(μ-CO)(μ_3-η^2-OPN(^{i}Pr)$_2$(μ_4-η^2-CCPh) **2a**

Bond lengths (Å)			
W–Ru(2)	2.7823(3)	W–Ru(1)	2.9248(3)
W–C(1)	2.050(3)	W–O(1)	1.7589(24)
W–O(2)	2.0743(21)	Ru(2)–Ru(1)	2.8428(4)
Ru(2)–Ru(3)	2.8802(4)	Ru(2)–Ru(4)	2.7587(4)
Ru(2)–C(1)	2.149(3)	Ru(1)–Ru(4)	2.8306(4)
Ru(1)–O(1)	2.2270(24)	Ru(3)–Ru(4)	2.6882(4)
Ru(4)–C(2)	2.279(3)	Ru(4)–C(1)	2.244(3)
P–O(2)	1.570(3)	P–N	1.641(3)
C(2)–C(1)	1.374(4)		
Bond angles (°)			
O(1)–W–O(2)	96.53	W–O(2)–P	97.62(11)
W–P–O(2)	48.09(8)	O(2)–P–N	106.10(14)
Torsion angle (°)			
Ru3–Ru2–Ru4–Ru1	177.43		

solution. Full matrix least-squares refinements minimized the function: $\Sigma_{hkl} w(|F_o| - |F_c|)^2$ where $w = 1/\sigma(F_o)2$, $\sigma(F_o) = \sigma(F_o^2)/2F_o$ and $\sigma(F_o^2) = [\sigma(I_{raw})^2 + (0.02I_{net})^2]^{1/2}/Lp$.

The crystallographic space group $P2_1/n$ was uniquely identified for compound **2a** by the pattern of systematic absences observed during the collection of intensity data. For compounds **3a** and **4a** the space group $P\bar{1}$ was assumed and confirmed by successful solution and refinement of the structure. All structures were solved by a combination of direct methods (SOLVER) and difference Fourier syntheses. All non hydrogen atoms were refined with anisotropic thermal parameters.

Table 3
Selective intramolecular bond lengths (Å) and angles (°) for η^5-Cp*W(μ-O)$_2$$Ru_4(CO)_{10}$($\mu_3$-PN(^{i}Pr)$_2$($\mu_4$-$\eta^2$-CCPh) **3a**

Bond lengths (Å)			
W–Ru(1)	2.6910(5)	W–Ru(2)	3.0467(5)
W–O(2)	1.783(4)	W–O(1)	1.815(4)
W–C(1)	2.770(5)	W–C(2)	2.099(5)
Ru(4)–Ru(1)	2.8661(6)	Ru(4)–Ru(3)	2.8393(7)
Ru(4)–P	2.3124(14)	Ru(4)–C(1)	2.470(5)
Ru(1)–Ru(2)	2.8154(7)	Ru(1)–O(1)	2.147(4)
Ru(1)–C(1)	2.136(6)	Ru(1)–C(2)	2.231(5)
Ru(2)–Ru(3)	2.7786(6)	Ru(2)–P	2.2535(14)
Ru(2)–O(2)	2.191(4)	Ru(2)–C(1)	2.235(5)
Ru(3)–P	2.4803(15)	Ru(3)–C(1)	2.059(6)
P–N	1.643(5)	C(1)–C(2)	1.406(8)
Ru(2)–Ru(4)	3.647(6)	Ru(3)–Ru(1)	3.981(6)
Bond angle (°)			
O(2)–W–O(1)	110.98(18)		
Torsion angles (°)			
Ru3–Ru4–Ru2–Ru1	134.72(5)		
Ru1–W–Ru2–Ru4	59.98(2)		

Table 4
Selective intramolecular bond lengths (Å) and angles (°) for η^5-Cp*WF(μ-O)H$Ru_4(CO)_{10}$[μ_3-η^2-P(O)N(^{i}Pr)$_2$](μ_4-η^2-CCPh) **4a**

Bond lengths (Å)			
Ru(1)–Ru(3)	2.7857(5)	Ru(1)–Ru(4)	2.7685(4)
Ru(1)–W	2.8740(4)	Ru(2)–Ru(3)	2.7686(4)
Ru(2)–O(1)	2.0612(23)	Ru(3)–Ru(4)	2.9271(4)
Ru(3)–W	2.8895(4)	Ru(3)–O(1)	2.1164(22)
Ru(3)–C(1)	2.167(3)	Ru(4)–C(2)	2.072(3)
W–F	1.9731(19)	W–O(1)	1.9549(23)
W–O(2)	2.1166(22)	W–C(1)	1.966(3)
P–N	1.640(3)	P–O(2)	1.5586(25)
C(1)–C(2)	1.401(5)		
Bond angle (°)			
O(1)–W–O(2)	80.81(9)		

4. Supplementary material

Texts describing the experimental details for complexes **2a**, **3a** and **4a**, full details of crystal structure analyses including tables of bond distances and angles, atomic coordinates, anisotropic thermal parameters (29 pages). This material is available from the authors on request.

Acknowledgements

This work was supported by grants from the National Research Council of Canada and the Natural Sciences and Engineering Research Council of Canada (to A.J.C.). We are very grateful to Professor Y. Chi for a sample of Cp*W(O)$_2$C$_2$Ph.

References

[1] (a) W.P. Griffith, Coord. Chem. Rev. 5 (1970) 459. (b) B. Jezowska-Trzebiatowska, Pure Appl. Chem. 27 (1971) 89. (c) W.A. Herrmann, E. Herdtweck, M. Filoel, J. Kulpe, U. Kusthardt, J. Okuda, Polyhedron 6 (1987) 1165. (d) Y. Chi, L.-S. Hwang, G.-H. Lee, S.-M. Peng, J. Chem. Soc. Chem. Commun. (1988) 1456. (e) F. Bottomley, L. Sutin, Adv. Organomet. Chem. 28 (1988) 339. (f) C.K. Schauer, E.J. Voss, M. Sabat, D.F. Shriver, J. Am. Chem. Soc. 111 (1989) 7662. (g) B.O. West, Polyhedron 8 (1989) 219. (h) F. Bottomley, Polyhedron 11 (1992) 1707. (i) C.-M. Che, V.W.-W. Yam, Adv. Inorg. Chem. 39 (1992) 233. (j) J. Xiao, J.J. Vittal, R.J. Puddephatt, L. Manojlovic-Muir, K.W. Muir, J. Am. Chem. Soc. 115 (1993) 7882. (k) W.A. Herrmann, P.W. Roesky, M. Wang, W. Scherer, Organometallics 13 (1994) 4531.

[2] (a) Y. Chi, J.R. Shapley, J.W. Ziller, M.R. Churchill, Organometallics 6 (1987) 301. (b) J.R. Shapley, J.T. Park, M.R. Churchill, J.W. Ziller, L.R. Beanan, J. Am. Chem. Soc. 106 (1984) 1144. (c) Y. Chi, J.R. Shapley, M.R. Churchill, J.C. Fettinger, J. Organomet. Chem. 372 (1989) 273. (d) N.S. Lai, W.C. Tu, Y. Chi, S.-M. Peng, G.-H. Lee, Organometallics 13 (1994) 4653. (e) Y. Chi, L.-S. Hwang, G.-H. Lee, S.-M. Peng, J. Chem. Soc. Chem. Commun. (1988) 1456. (f) H.L. Wu, G.L. Lu, Y. Chi, L.J. Farrugia, S.-M. Peng G.-H. Lee, Inorg. Chem. 35 (1996) 6015.

[3] J. Xiao, R. Puddephatt, J. Coord. Chem. Rev. 143 (1995) 457.
[4] P. Blenkiron, A.J. Carty, S.-M. Peng, G.-H. Lee, C.-J. Su, C.-W. Shiu, Y. Chi, Organometallics 16 (1997) 519.
[5] C.-W. Shue, C.-J. Su, C.-W. Pin, Y. Chi, S.-M. Peng, G.-H. Lee, J. Organomet. Chem. 545–546 (1997) 151.
[6] (a) J. Lunniss, S.A. MacLaughlin, N.J. Taylor, A.J. Carty, E. Sappa, Organometallics 4 (1985) 2066. (b) J.F. Corrigan, S. Doherty, N.J. Taylor, A.J. Carty, Organometallics 11 (1992) 3160. (c) J.F. Corrigan, S. Doherty, N.J. Taylor, A.J. Carty, Organometallics 12 (1993) 1365. (d) P.J. Low, G.D. Enright, A.J. Carty, J. Organomet. Chem. 565 (1998) 279.
[7] P.-C. Su, S.-J. Chiang, L.-L. Chang, Y. Chi, S.-M. Peng, G.-H. Lee, Organometallics 14 (1995) 4844.
[8] W. Wang, J.F. Corrigan, S. Doherty, G.D. Enright, N.J. Taylor, A.J. Carty, Organometallics 15 (1996) 2770.
[9] (a) J.F. Corrigan, S. Doherty, N.J. Taylor, A.J. Carty, J. Am. Chem. Soc. 116 (1994) 9799. (b) W. Wang, A.J. Carty, New J. Chem. 21 (1997) 773. (c) W. Wang, G.D. Enright, J. Driediger, A.J. Carty, J. Organomet. Chem. 541 (1997) 461.
[10] (a) N.M. Doherty, N.W. Hoffman, Chem. Rev. 91 (1991) 553. (b) E.F. Murphy, M. Ramaswamy, H.W. Roesky, Chem. Rev. 97 (1997) 3425.
[11] D.M. Dawson, R.A. Henderson, A. Hills, D.L. Hughes, J. Chem. Soc. Dalton Trans. (1992) 973.
[12] D. Buchholz, G. Huttner, W. Imhof, J. Organomet. Chem. 388 (1990) 307.
[13] (a) J.F. De Wet, M.R. Caire, B.J. Gellatly, Acta Crystallogr. B 34 (1978) 762. (b) S.Z. Goldberg, K.N. Raymond, Inorg. Chem. 12 (1973) 2923.
[14] G. Wulfsberg, Principles of Descriptive Inorganic Chemistry, University Science Books, Mill Valley, 1990, Table 6.4, p. 447.
[15] (a) M. Cousins, M.L.H. Green, J. Chem. Soc. A (1969) 16. (b) G. Ciani, A. Sironi, V.G. Albano, J. Chem. Soc. Dalton Trans. (1977) 1667. (c) F. Bottomley, D.E. Paez, H.P. Frritz, J. Am. Chem. Soc. 103 (1981) 5581. (d) A. Bino, F.A. Cotton, Z. Dori, B.S.W. Kolthammer, J. Am. Chem. Soc. 103 (1981) 5779. (e) F. Bottomley, D.E. Paez, L. Sutin, P.S. White, J. Chem. Soc. Chem. Commun. (1985) 597. (f) F. Bottomley, D.F. Drummond, G.O. Egharevba, P.S. White, Organometallics 5 (1986) 1620. (g) J.L. Davidson, K. Davidson, W.E. Lindsell, N.W. Murall, A.J. Welch, J. Chem Soc. Dalton. Trans. (1986) 1677. (h) C.P. Gibson, J.-S. Huang, L.F. Dahl, Organometallics 5 (1986) 1676. (i) A. Colombie, J.-J. Bonnet, P. Fomppeyrine, G. Lavigne, S. Sunshine, Organometallics 5 (1986) 1154. (j) U.A. Jayasoriya, C.E. Anson, J. Am. Chem. Soc. 108 (1986) 2894. (k) G. Lin, W.T. Wang, Polyhedron (1995) 3167.
[16] J.H. Yamamoto, A.J. Carty, unpublished results.
[17] E.J. Gabe, Y. Le Page, J.P. Charland, F.L. Lee, P.S. White, J. Appl. Crystallogr. 22 (1989) 384.
[18] International Tables for X-ray Crystallography, vol. IV, Table 2.2B, Kynoch Press, Birmingham, UK, 1975, pp. 99–101.
[19] International Tables for X-ray Crystallography, vol. IV, Table 2.3.1, Kynoch Press, Birmingham, UK, 1975, pp. 149–150.